

# Design of tunable terahertz photonic crystal narrow-band filters\*

ZHANG Hui (张会)\*\*, BAI Jin-jun (白晋军), GUO Peng (郭澎), WANG Xiang-hui (王湘晖), and CHANG Sheng-jiang (常胜江)

*Institute of Modern Optics, Nankai University, Tianjin 300071, China.*

(Received 16 January 2009)

The coupling between the line defect and point defect in a two-dimensional photonic crystal is studied by using plane wave expansion method and finite difference time domain method. Based on the analysis, we propose a novel tunable terahertz narrow-band filter. Simulation results on the defect modes and output spectra show that the photonic crystal that consists of two line defects and one point defect can act as a tunable filter with narrow bandwidth of 0.02 THz under the control of an external electric field.

**Document code:** A **Article ID:** 1673-1905(2009)03-0169-4

**DOI** 10.1007/s11801-009-8127-6

Terahertz (THz) wavelengths that cover the range of 30  $\mu\text{m}$ -3  $\mu\text{m}$ , used to be the research gap between microwave and infrared regions. In recent years, the stable ultra-fast lasers have dramatically accelerated the improvements in the generation and detection of THz radiation<sup>[1]</sup>. Since THz radiation lies in the region which predominantly excites vibrational modes and may extend to the rotational modes at lower frequencies and shows small absorption in some non-polar materials including plastic and china, it has attracted more and more attentions, and it also has the potential applications for the biological imaging and sensing<sup>[2]</sup>, detection of explosive<sup>[3]</sup>, spectroscopy<sup>[4]</sup>, and high speed communication<sup>[5]</sup>. For these applications, the functional devices including switches, filters, modulators and polarizers are indispensable for the realization of a practical system<sup>[6,7]</sup>. In particular, the narrow-band filters are crucial for the THz communication and multi-spectral imaging.

Photonic crystals (PCs), in which dielectric materials are periodically arrayed in one or more dimensions, are successful in controlling and propagating electromagnetic waves including millimeter, visible light and THz waves. Since the lattice constant of PCs is proportional to the wavelength of the incident electromagnetic waves, it is easier to fabricate PCs devices in the THz wave band. Up to now, there are some reports about THz filters. Nemeč et al.<sup>[8]</sup> reported a one-dimensional PCs-based THz filter working from 267 GHz (at 290 K) down to 220 GHz (at 170 K). Krumbholz et

al.<sup>[9]</sup> proposed an omnidirectional high-reflectivity THz mirror in the frequency band between 319 GHz and 375 GHz. However, there are few papers dealing with the tunable narrow-band filters working in higher frequency.

In this letter, the coupling properties between the line defect and point defect of PCs in THz wave band are studied by using the plane wave expansion (PWE) and finite difference time domain (FDTD) method. A tunable narrow-band filter that consists of two waveguides and a cavity filled with nematic liquid crystal (LC) in PCs is proposed. The electrically controlled LC is used to realize tunable ability as a narrowband filter.

Generally, the two-dimensional PCs have three typical lattices: square, hexagonal and honeycomb lattices. In this letter, the PC with the square lattice of silicon rods in air is studied since this structure can generate relative large TM photonic bandgap (PBG). The dielectric constant of silicon with high resistivity is 11.7<sup>[10]</sup>. There are a number of ways to produce defect in PCs, for example, one or several rows of rods are devoid so as to form line defects, and one rod is removed or changed in size or material properties so as to form point defect. Line and point defects are the most important elements for PCs functional devices. The line defects have continuous defect modes in a range of frequency while the point defects have one or several discrete defect modes in certain frequencies. Although the defects can confine the defect modes in themselves, there are energy coupling be-

\* This work has been supported by the National Basic Research Program of China (Grant No.2007CB310403), the National Natural Science Foundation of China (Grant No. 60772105), and Key Program of the Applied Basic Research of Tianjin(Grant No. 07JCZDJC05500)

\*\* E-mail: zhanghuizxh@126.com

tween the defects.

LC (E7) is an uniaxial anisotropic medium in which the principal axis can be rotated under the control of external electric field. The ordinary and the extra ordinary refractive index  $n_o, n_e$  of E7 measured with THz time-domain spectroscopy system at 1 THz are about  $n_o = 1.57$  and  $n_e = 1.75$ , respectively<sup>[11]</sup>. We assume that LC is filled in a silicon tube with such a small wall thickness that can be neglected. Because of the interaction between the tube internal wall and the molecule of LC, the initial direction of the principal axis of E7 is parallel to the tube direction i.e. the y-axis direction<sup>[12]</sup>. The threshold field (the Freedericksz transition) required for reorienting the E7 molecules along the external electric field is defined as:

$$E_{th} = (\pi / L)(k_3 \varepsilon_a \varepsilon_0)^{1/2}, \quad (1)$$

where  $k_3, \varepsilon_a$  and  $\varepsilon_0$  are the bend elastic constant, dielectric anisotropy, and electric permittivity of free space, respectively. For our device, the threshold field is calculated as  $E_{th} = 11.7$  V/cm. When the electric field intensity increases, the effective refractive index can be written as<sup>[13]</sup>

$$\frac{1}{n_{eff}^2(\theta)} = \frac{\sin^2(\theta)}{n_e^2} + \frac{\cos^2(\theta)}{n_o^2}, \quad (2)$$

where  $\theta$  is the reorientation angle of LC molecules from the initial orientation.

We first investigate the defect mode of a line defect in PCs with square lattice by using PWE method. Line defects are periodic in one dimension, so PWE method can not be directly applied to calculate the defect modes since it is applicable only for the structures that are periodic in two dimensions. In order to use PWE to calculate the defect mode, we assume that the line defect has a long period in the other dimension and the super-cell method can be applied. In our calculations, the super cell dimension is chosen to be 9 to ensure the precision requirement, as shown in the inset of Fig.1. The PBG dispersion relation and defect mode of the line defect in PC are shown in Fig.1, in which the eigenvalues in normalized frequency for different values of wave vector ( $K_{norm} = k_x a/2\pi$ ) are given. The blank area between the range of 0.24-0.44 without eigen-frequencies represents the PBG of the PC with line defect. The data denoted by asterisk in the PBG is the defect mode of the line defect, whose frequency exists within 0.305-0.434 in normalized frequency, (converted to 0.915THz -1.302 THz). The frequencies of the defect modes are the transmitting frequencies in the line defect. The THz wave with other frequencies will be reflected and can not be guided in the line defect.

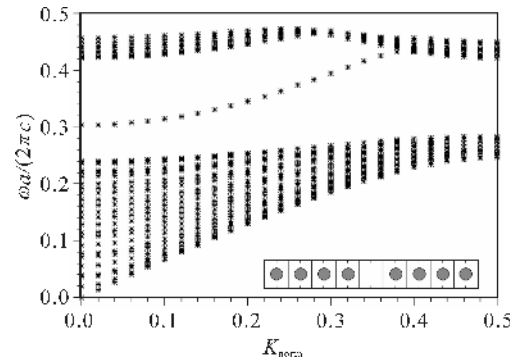


**Fig.1 The photonic bandgap dispersion and defect mode of the waveguide**

Fig.2 shows the defect mode of a point defect filled with E7. The super cell is shown in the right side of Fig.2, in which the black round represents the point defect filled with E7 in the condition that the refractive index and radius of the point defect are 1.57 and  $R_1 = 0.2 a$ , respectively. There is no defect mode dispersion for point defect and the defect mode exists only for a certain frequency, which is 0.355 in normalized frequency (converted to 1.065 THz), as shown in Fig.2. When the radius of the point defect increases, the frequency of the defect mode decreases, and as the radius of the point defect is larger than  $0.52 a$ , the defect mode becomes multi-mode with two different frequencies as shown in Fig.3. The multi-mode of the point defect has straightforward and potentially promising applications in wavelength division multiplex system.

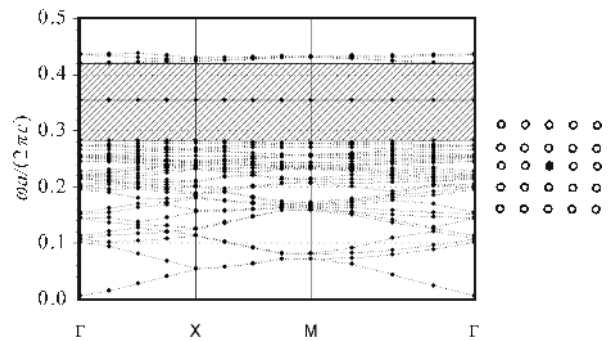


**Fig.2 The defect mode of the point defect filled with liquid crystal**

The principal axis of the LC molecules will rotate towards the  $x$  axis when the intensity of external electrical field increases. This will result in the change of the effective refractive index of LC from  $n_o$  to  $n_e$ . Therefore, we further study the defect modes as the refractive index of the point defect

changes from 1.57 to 1.75. Fig.4 shows the normalized frequency variation of the defect modes with the refractive index difference ( $\sigma_1$ ) between the point defect and the air background. It can be seen that the frequency of defect modes decreases from 0.355 (1.065 THz) to 0.345 (1.035 THz) in normalized frequency when  $\sigma_1$  increases from 1.57 to 1.75.

Overall, the frequencies of the point defects lie in the frequency region of the line defect mode. If the line defect is initially excited, modes which are equal to the point defect modes will preferentially be resonated, energy coupling between them will occur.

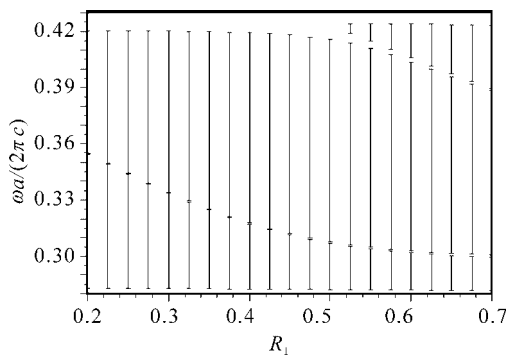


**Fig.3 The variation of the defect modes with the radius of the defect**

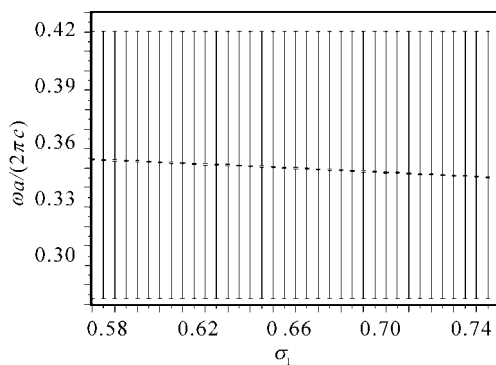


**Fig.4 The variation of the defect modes with the refractive index of the defect**

Based on the analysis above, we design a tunable narrow-band filter, which is composed with an up-loading line defect A, a point defect C and a down-loading line defect B, as shown in Fig.5. The E7-filled point defect with  $R_1 = 0.3 a$  is the key element of the filter. It can pick up a mode from the line defect A and couple the energy of this frequency into the line defect C. The resonance mode of the point defect can be tuned by the birefringence of LC under the control of external electrical field, which is generated by two electrodes placed on both sides of the PC.

The output spectra from the line defect B are analyzed by

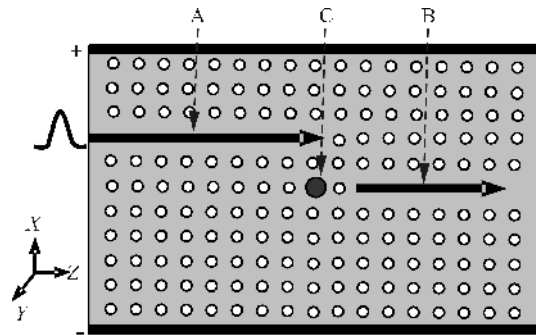


**Fig.5 Design of the tunable narrow-band filter**

using the FDTD method with the perfectly matched layer (PML) absorbing boundary condition. The Gaussian pulse, whose central normalized frequency is at 0.3125 (converted to 0.96 THz) and bandwidth is 0.36 THz, is launched into the up-loading waveguide A. Fig.6 shows the launched pulse spectrum (solid curve), the output spectrum (dashed curve) under the condition that the refractive index of point defect is 1.57 and the output spectrum (dotted curve) under the condition that the refractive index of point defect is 1.75. The central normalized frequency and bandwidth are 0.332(0.996 THz) and 0.017 THz when the electric field is less than the threshold field and thus the effective refractive index of LC is 1.57. As the electric field is so much larger than the threshold field that the effective refractive index of LC reaches to 1.75, the central normalized frequency and bandwidth are 0.3133 (0.94 THz) and 0.020 THz, respectively. It can be seen that the central frequency decreases when the electric field increases.

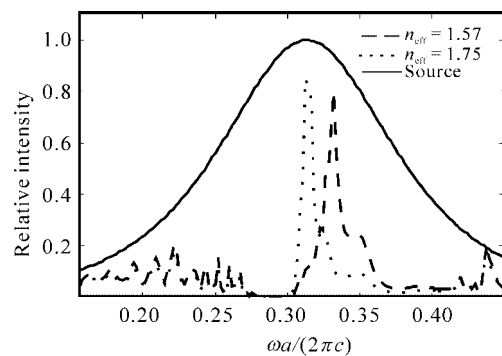


**Fig.6 The output narrow-band spectra**

In conclusion, we have designed a tunable narrow-band filter, which central frequency can be tuned from 0.94 THz to 0.966 THz by using the birefringence of LC under the control of external electric field. The bandwidth of the filter is 0.02 THz.

## References

- [1] Schneider A, Stillhart M, and Gunter P, *Opt. Express*, **14** (2006), 5376.
- [2] HE Zhi-hong, YAO Jian-quan, and REN Xia, *Journal of Optoelectronics • Laser*, **19** (2008), 34.(in Chinese)
- [3] Federici J F, Schulkin B, Huang F, Gary D, Barat R, Oliveira F, and Zimdars D, *Semicond. Sci. Technol.*, **20** (2005), 266.
- [4] Pickwell E, and Wallace V P, *Appl. Phys.*, **39** (2006), 301.
- [5] Costa D B da and Yacoub M D, *Electr.Lett.*, **44** (2008), 214.
- [6] Li J, He J and Hong Z, *Appl. Opt.*, **46** (2007), 5034.
- [7] Kleine-Ostmann T, Dawson P, Pierz K, Hein G and Koch M, *Appl. Phys.Lett.*, **84** (2004), 3555.
- [8] Nemeč H, Duvillaret L, Garet F, Kuzel P, Xavier P, Richard J and Rauly D, *J. Appl. Phys.*, **96** (2004), 4072.
- [9] Krumbholz N, Gerlach K, Rutz F, Koch M, Piesiewicz T, Kurner T, and Mittleman D, *Appl. Phys. Lett.*, **88** (2006), 202905.
- [10] Hu X, Jiang P and Gong Q, *Appl. Phys. B*, **87** (2007), 57.
- [11] Chen C Y, Hsieh C F, and Lin Y F, *Opt. Express*, **12** (2004), 2630.
- [12] Wu H Y, Hsieh C F and Tang T T, *IEEE Photonics Tech. Lett.*, **18** (2006), 1488.
- [13] Knight J C, Birks T A and Russell P St J, *Opt. Lett.*, **21**(1996), 1547.